

Investigations of a ^{99m}Tc -Labeled Bacteriophage as a Potential Infection-Specific Imaging Agent

Mary Rusckowski, PhD; Suresh Gupta, PhD; Guozheng Liu, PhD; Shuping Dou, BS; and Donald J Hnatowich, PhD

Division of Nuclear Medicine, Department of Radiology, University of Massachusetts Medical School, Worcester, Massachusetts

Because bacteriophages (phages) have a natural specificity for bacteria, it may be possible to develop radiolabeled phages as infection-specific agents. **Methods:** The M13 phage was radiolabeled with ^{99m}Tc via mercaptoacetyl triglycine and purified by polyethylene glycol precipitation. After radiolabeling, the phage was tested for binding at 1, 5, and 10 min to *Escherichia coli* strain 2537, *E. coli* strain 25922, and *Staphylococcus aureus* strain 29213. The radiolabeled phage was also tested for specificity in mouse models that had received a subcutaneous injection of either live (infection/inflammation model) or heat-inactivated (inflammation model) cultures in a thigh. The labeled phage (10^9 plaque-forming units, 1–3.7 MBq) was administered either within 20 min (to minimize the contribution from inflammation) or 3 h after induction. The animals were killed 3 h later.

Results: The radiochemical purity of the labeled phage exceeded 95% by strip chromatography using instant thin-layer chromatography/acetone and paper/saline. Binding of the labeled phage to each of the 3 bacterial strains in vitro was immediate, reaching a maximum at 1 min. However, the percentage bound was significantly higher ($P = 0.0008$) for *E. coli* 2537 than for either of the other 2 bacteria (84% vs. 41% and 48%). Furthermore, binding to *E. coli* 2537 was unchanged at 10 min, whereas binding to both *E. coli* 25922 and *S. aureus* decreased to 33%. At 3 h in vivo, the ratio of target thigh to normal thigh was significantly higher ($P \leq 0.017$) in the infection/inflammation model (2 to 2.5 fold) than in the inflammation model (1.5 to 1.8) and therefore suggestive of increased accumulation specific to infection. The difference was slightly more pronounced in animals that received labeled phage at 20 min after inoculation, showing a ratio of 2.3 for infected thigh to normal thigh and a ratio of 1.6 for inflamed thigh to normal thigh. Although absolute uptake was lowest in the infection/inflammation thigh of mice infected with *E. coli* 2537, this finding was presumably due to the therapeutic effect of the phage on this strain. **Conclusion:** Radiolabeled bacteriophages should be further investigated as potential agents for specific imaging of infection.

Key Words: ^{99m}Tc -bacteriophage; infection imaging; bacterial infection

J Nucl Med 2004; 45:1201–1208

There remains today an acute need in nuclear medicine for a diagnostic agent that can distinguish between infection and sterile inflammation. To quote from a seminal article on infection imaging, “the need for techniques for anatomically delineating the primary and metastatic sites of infection; the need for noninvasive imaging techniques that could be performed repetitively to assess the response to therapy; the need for a noninvasive technique for in vivo, specific diagnosis that would obviate the need for invasive biopsy procedures; and the need for targeted therapy of such infections as those caused by fungi that would permit more aggressive therapy of the process with lesser amounts of systemic toxicity” exist for patients with infection (*1*). Although this statement was published almost 15 y ago, the same critical need for infection-specific imaging exists today. As one important example, the precise microbial cause remains undefined in approximately 30% of patients presenting with community-acquired pneumonia, one of the most common infections that lead to hospitalization. This inability to define the precise cause of infection leads clinicians to treat with very broad spectrum antibiotic therapy as opposed to targeted treatment for patients with suspected pneumonia. Overuse of antibiotic treatment because of this type of “shotgun” approach is a leading factor in the development of bacterial resistance to antibiotics. Obviously, a radiolabeled agent that could target specific bacterial pathogens both to confirm the presence of pneumonia and to define the precise etiology would be of considerable value. Another important example may be suspected infection of prosthetic joints, a devastating complication that usually results in the need for removal of the prosthesis, a prolonged course of antibiotic therapy, and then reimplantation of a new prosthesis. In this situation, the most frequent pathogens are normal skin flora, and even with direct aspiration of the joint it can be difficult to determine whether bacteria identified on culture of synovial fluid represent true infection or inadvertent contamination of the sample during collection. By using radiolabeled agents with specificity for the 2 or 3 possible bacteria responsible for most infections, it should be possible to precisely identify the bacterium so that effective therapy can be initiated without the need for the broad-spectrum antibiotic therapy that only encourages the

Received Oct. 9, 2003; revision accepted Mar. 19, 2004.

For correspondence or reprints contact: Mary Rusckowski, PhD, Division of Nuclear Medicine, Department of Radiology, University of Massachusetts Medical School, Worcester, MA 01655-0243.

E-mail: mary.rusckowski@umassmed.edu

development of resistance (R. Ellison, oral and written communication, August 2003).

Agents with documented specificity for bacteria may be appropriate choices for imaging those bacteria. Two such agents currently under investigation are Infecton, a ^{99m}Tc -labeled ciprofloxacin antibiotic (2–5), and ^{99m}Tc -labeled peptide fragments of ubiquicidin, an antimicrobial peptide (6–8). Most of the work with Infecton has been clinical, and several successful studies have been reported, whereas the work with ubiquicidin has been limited to animal models.

Bacteriophages (phages) are viruses that show no specificity for mammalian cells and infect bacteria exclusively. Phages bind to bacterial cells by attaching to specific surface receptors and, by inserting their genetic material into the cell, use the bacteria as a host for reproduction. Phages have been used clinically to treat bacterial infections since the 1920s (9); thus, they are presumably nontoxic, although their safety and efficacy have yet to be validated. Their clinical use declined, particularly in the West, after the development of antibiotics. Because of this natural specificity of phages for bacteria, phages may be useful for detecting bacterial infections through imaging. Most phages infect several bacterial species but show a range of specificity that is more narrow than that exhibited by antibiotics. For example, some phages show specificity only toward a single bacterial strain (10). Therefore, unlike the case with radiolabeled antibiotics, it may be possible to select a radiolabeled phage specific to a suspected bacterial infection but without specificity for natural endogenous bacteria.

This report describes what may be the first investigation of a radiolabeled phage as a potential diagnostic imaging agent for bacterial infection. After radiolabeling with ^{99m}Tc , we have used the bacteriophage M13 as a test phage to evaluate binding affinity in vitro in bacteria and in vivo in an infection/inflammation mouse model. The M13 phage was selected as a well-characterized common laboratory phage known to be infectious to common bacteria such as the 2 *Escherichia coli* strains used in this investigation. The objectives of this investigation were to determine the stability of ^{99m}Tc on the phage when radiolabeled via mercaptoacetyltriglycine (MAG3), to determine the fate of the radiolabeled phage infecting both live and heat-killed bacteria, and, finally, to help establish whether imaging with the radiolabeled phage may be used to distinguish infection from inflammation.

MATERIALS AND METHODS

The M13 phage and *E. coli* strain 2537 were obtained from New England Biolabs, Inc. A second *E. coli* strain (25922) and *Staphylococcus aureus* strain 29213 were obtained as plate cultures from the Clinical Microbiology Department at this university. Luria-Bertani (LB) medium containing Bacto-Tryptone (Sigma-Aldrich), yeast extract (Sigma), and NaCl was prepared according to standard procedures and autoclaved. The *S*-acetyl *N*-hydroxysuccinimide (NHS)-MAG3 was synthesized in house (11), and the structure was confirmed by elemental analysis, proton nuclear

magnetic resonance, and mass spectroscopy. The ^{99m}Tc -pertechnetate was eluted from a ^{99}Mo – ^{99m}Tc generator (Perkin-Elmer). All other chemicals were used as supplied. Male CD-1 mice weighing 22–25 g were obtained from Charles River Laboratories.

Stocks of the 3 bacterial strains were grown and maintained as plate cultures and stored at 4°C. The day before each study, liquid cultures in LB medium were seeded and grown overnight at 37°C while shaking at 250 rpm. Bacteria were counted using a hemacytometer and diluted in LB medium for use. To prepare the infection/inflammation model, aliquots of the bacterial cultures were diluted in LB medium to a concentration of 4.8×10^8 cells/mL, and 0.1 mL was administered subcutaneously in one thigh of each of the CD-1 mice. To prepare the inflammation model, the diluted bacterial preparations (4.8×10^8 /mL) were heated in a boiling water bath for 30 min, sonicated for 10 min, and then spun at 8,200g for 3 min (Biofuge-15; Heraeus Instruments). No growth was apparent 1 d after samples were plated on LB agar, indicating sterility. As before, 0.1 mL of the cell-free broth was administered subcutaneously in a thigh.

Preparation of Phage

The M13 phage was propagated in *E. coli* 2537 using standard methods (12). In brief, a liquid culture of the *E. coli* was diluted 1:100 with 20 mL of LB medium to which 10 μL of the stock phage (2×10^{11} plaque-forming units [PFU]) were added. After 4.5 h of vigorous shaking at 37°C, the sample was spun at 1,400g (model CR 412; Jouan) for 10 min to pellet the bacteria. The supernatant was spun again and then transferred to a fresh tube, and a solution of polyethylene glycol 8000 20% w/v and 2.5 mol/L NaCl (PEG/NaCl) was added at a ratio of 1:6 (v/v) (13). After the sample was spun at 15,000g for 20 min, the phage pellet was recovered and suspended in Dulbecco's phosphate-buffered saline (PBS) (Invitrogen Corp.). The precipitation was repeated with the PEG/NaCl solution. The final phage pellet was suspended in PBS and stored at 4°C.

Conjugation of M13 Phage with MAG3

The phage were conjugated with *S*-acetyl NHS-MAG3 using methods standard in this laboratory for the ^{99m}Tc radiolabeling of proteins, peptides, and oligomers (14). In brief, to 50–100 μL of PBS containing about 10^{10} PFU/ μL of phage were added 2–4 μL of a 0.1 mol/L solution of sodium bicarbonate solution, pH 9.0, for a final pH of 8.0. With constant agitation, 2–4 μL of a fresh solution of NHS-MAG3 in dry DMF (1 mg/mL) were also added. The volume of DMF was always less than 10% of the final volume. The conjugation mixture was incubated at room temperature for 45 min. Unbound MAG3 was then removed by precipitation of the phage with the PEG/NaCl solution as before, and the sample was spun at 15,000g for 15 min at 4°C to pellet the phage. The MAG3-phage pellet was suspended in 50–100 μL of PBS and purified once again by reprecipitation with PEG/NaCl. The final pellet of conjugated phage was suspended in PBS and stored at 4°C.

Radiolabeling of MAG3 Phage with ^{99m}Tc

For ^{99m}Tc radiolabeling, an aliquot of sodium tartrate (50 mg/mL) in sodium bicarbonate (0.5 mol/L), ammonium acetate (0.25 mol/L), and ammonium hydroxide 0.175 mol/L buffer (pH 9.2) was added to the MAG3 phage (5–50 μL ; concentration $\sim 10^9$ PFU/ μL) so that the final concentration of tartrate was 7 $\mu\text{g/mL}$ in the labeling mixture. After addition of 9.25–37 MBq of ^{99m}Tc -pertechnetate generator eluent, 2 μL of a fresh solution of

$\text{SnCl}_2 \cdot 2\text{H}_2\text{O}$ (1 mg/mL in 10 mmol/L HCl) were added. The labeling mixture was incubated at room temperature for 30–60 min. The $^{99\text{m}}\text{Tc}$ -labeled MAG3 phage was purified by precipitation twice with PEG/NaCl as described above. Radiochemical purity was estimated by instant thin-layer chromatography (ITLC) with acetone as the solvent (ITLC-SG; Gelman) and by paper chromatography (Whatman no. 1; VWR) with saline as the solvent. Both radiolabeled phage and colloids remain at the origin in both systems, whereas pertechnetate, labeled tartrate, and MAG3 migrate in saline and only pertechnetate migrates in acetone. The chromatography strips were cut into 1 cm sections, and the radioactivity was determined in a γ well counter (Cobra II Auto-Gamma; Packard Instrument Co.). As a control, the identical labeling procedure was performed on phage that had not been conjugated with MAG3.

Stability of $^{99\text{m}}\text{Tc}$ -Phage in Serum and Buffer

To test the stability of the label on free phage, the $^{99\text{m}}\text{Tc}$ -labeled phage (20 μL , 4×10^{10} PFU) was added to 0.2 mL of fresh human serum or PBS at 37°C and aliquots were removed in duplicate at 15 min, 30 min, 1 h, 3 h, and 18 h for analysis by ITLC/acetone and paper/saline.

Binding of $^{99\text{m}}\text{Tc}$ -Phage to Bacteria

Binding of the labeled phage to bacteria was measured after the addition of $^{99\text{m}}\text{Tc}$ -phage (3.5×10^7 PFU) to 0.5 mL of each of the 3 strains at a cell count of $8 \times 10^8/\text{mL}$. Samples in triplicate were removed at 1, 5, and 10 min and spun at 8,200g for 3 min. The bacterial pellet was washed with PBS and counted for radioactivity.

Binding of $^{99\text{m}}\text{Tc}$ -Phage to Live and Heat-Killed Bacteria

To determine whether the $^{99\text{m}}\text{Tc}$ -phage bound to heat-killed bacteria, the labeled phage was incubated with both live and heat-killed preparations. The live bacterial preparations were adjusted to a concentration of $5.2 \times 10^8/\text{mL}$ in LB medium, each preparation was divided into 2 aliquots, and 1 aliquot was heated in a boiling water bath for 30 min for sterilization. All 6 preparations of live and heat-killed bacteria (0.5 mL of each) were incubated in duplicate in a 37°C water bath with the $^{99\text{m}}\text{Tc}$ -phage (3.5×10^6 PFU, about 0.011 MBq). After 5 min, the samples were spun at 8,200g for 3 min, the supernatant was removed, and the pellet was washed with PBS. The wash was pooled with the supernatant and counted in a γ well counter along with the pellets for associated activity.

Analysis of Supernatant Radioactivity

Because heat sterilization of bacteria is believed to damage the plasma membrane such that the cell constituents can escape, leaving membrane fragments (15), it was important in this study to establish whether the radiolabeled phage was retained on bacteria once the membranes were fragmented, in this case by heat denaturation. We wished to determine whether the phage remained bound to the bacterial cell wall or membrane fragments once the infected bacteria were killed. The method of analysis consisted of 2 serial centrifugations, a short spin to pellet bacteria and large fragments and their associated phage followed by a second spin to pellet smaller fragments. Preliminary studies showed the absence of free phage in these incubations (data not shown). As before, the labeled phage (10^9 PFU, about 0.011 MBq) was added to 4 mL of live and heat-killed *E. coli* preparations (each at $1.5 \times 10^9/\text{mL}$)

and incubated at 37°C. Samples were removed at 1, 15, and 60 min and spun at 850g for 1 min. The supernatants were then spun for a further 10 min at the same speed. The supernatants and pellets were then counted.

To obtain sufficient radioactivity for high-performance liquid chromatography (HPLC) analysis of the supernatant, this procedure was repeated but only on live bacteria and using phage radiolabeled at a higher specific activity. *E. coli* (6 mL at $5.2 \times 10^8/\text{mL}$) was incubated with $^{99\text{m}}\text{Tc}$ -phage (10^9 PFU, about 14.8 MBq) in a 37°C water bath as before, and samples were removed in duplicate at 1, 30, 60, and 105 min. To remove particulate matter, samples were first spun for 1 min at 1,000g and the supernatants were filtered through a 0.2 μm filter (13 mm Acrodisc; Gelman Sciences). The filtrate was analyzed by reversed-phase HPLC (C-18, YMC-pack ODS-AMQ, 4.6×250 mm; Waters) using a linear gradient at 1 mL/min going from 100% eluant A (0.1% trifluoroacetic acid in water) to 60% eluant B (0.1% trifluoroacetic acid in 90% acetonitrile/10% water) in 30 min. The unfiltered samples were analyzed by ITLC/acetone and paper/saline.

Biodistribution of $^{99\text{m}}\text{Tc}$ -Phage in Normal Mice

Biodistribution of the labeled phage was measured in normal CD-1 mice. About 0.1 mL, containing 2×10^9 PFU (about 1.18 MBq) of labeled phage, was administered to normal mice through a tail vein. Animals were sacrificed at 30 min, 3 h, 6 h, and 24 h ($n = 2$), and organs of interest and blood were removed, weighed, and counted in the γ well counter.

Infection and Inflammation in a Mouse Model

To help establish whether the labeled phage can be used to distinguish between infection and inflammation, normal mice were injected subcutaneously with each of the 3 live bacteria (infection/inflammation models) or sterilized cell-free broth (inflammation models) containing, most likely, bacterial debris and intracellular materials such as endotoxins. Mice received a subcutaneous injection of 0.1 mL of 1 of the 6 injectates ($n = 4$) into a thigh. At 3 h thereafter, mice received the labeled phage (10^9 PFU, about 1.036 MBq) through a tail vein, and after an additional 3 h, the animals were imaged on an APEX 409M large-view γ camera (Elscent). The study was also repeated with live and heat-killed preparations with only 20 min instead of 3 h between preparation of the model and administration of the labeled phage. The shorter period was selected in the hope of minimizing the contribution from inflammation in the infection/inflammation model. After imaging, the organs of interest and blood were removed, weighed, and counted in the γ well counter.

RESULTS

Radiolabeled Phage

Analysis by both ITLC and paper chromatography of all radiolabeled phage preparations showed greater than 90% of the label remaining at the origin, almost certainly as labeled phage (data not presented). Radioactivity binding to native phage without MAG3 was less than 5%.

Stability of Labeled Phage in Serum and Buffer

Figure 1 presents a histogram of the activity remaining at the origin on analysis by strip chromatography of labeled phage in serum and buffer over time. As shown, the label on

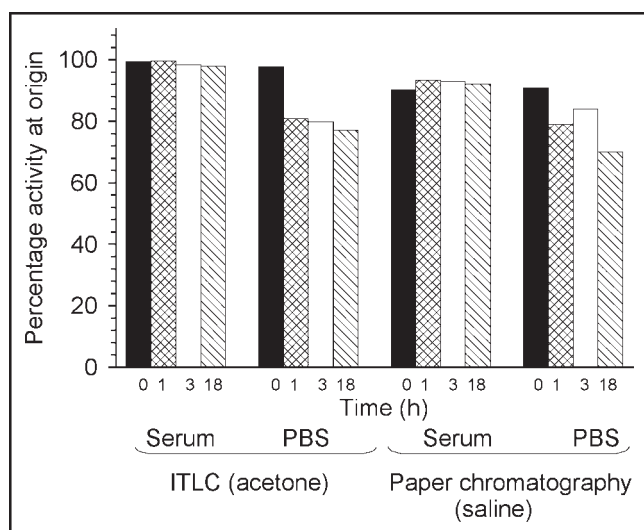


FIGURE 1. Histogram of activity remaining at the origin with ITLC in acetone and paper chromatography in saline of labeled phage in serum or buffer over time.

phage showed no important instabilities leading to migration in serum. At 18 h of incubation, 99% (ITLC) and 91% (paper) of the added activity still remained at the origin. The results in buffer were somewhat lower with 80% (ITLC) and 77% (paper) at 1 h but with minimal change over time thereafter. The radiolabeled phage was thus shown to be stable under the conditions of incubation, especially in serum.

Binding of ^{99m}Tc -Phage to Live and Heat-Killed Bacteria

When the labeled phage was added to the live bacterial suspensions, binding was immediate, as shown in Figure 2. As early as 1 min, $84\% \pm 2\%$ of the label was associated with *E. coli* 2537, and this percentage was unchanged over

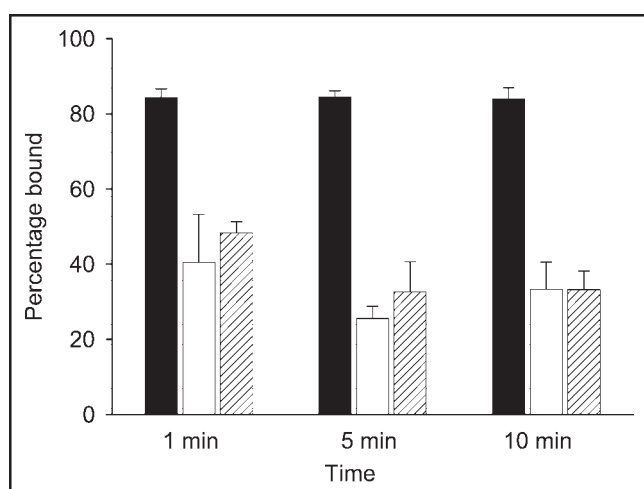


FIGURE 2. In vitro measure of ^{99m}Tc -MAG3-phage binding to bacteria. Percentage of added activity bound is shown for *E. coli* 2537 (black bars), *E. coli* 25922 (white bars), and *S. aureus* (hatched bars).

10 min. By contrast, *E. coli* 25922 and *S. aureus* bound only $41\% \pm 2\%$ and $48\% \pm 3\%$, respectively, at 1 min, followed by a slight decrease to $33\% \pm 6\%$ at 5 and 10 min in both cases. Thus, even though the labeled M13 phage showed preferential binding to a single *E. coli* strain, it also bound to a second strain and to *S. aureus*, although at a lower level.

Incubation of labeled phage with live and heat-killed bacteria demonstrated that the labeled phage bound almost equally to both regardless of bacterial strain. As shown in Table 1, although more radioactivity was associated with the live bacteria than with the heat-killed preparations, the difference was only about 11% irrespective of the bacterial type.

The radioactivity levels in the supernatant of these preparations were investigated further for *E. coli* 2537 by measurement after a second, longer, centrifugation. As shown in Table 2, in the case of the live bacteria, radioactivity in the supernatants was unchanged after the first short (1 min at 850g) and second longer (10 min at 850g) centrifugation. By contrast, in the case of the heat-killed bacteria considerably more radioactivity remained in suspension after the first centrifugation, and the level was brought down only after the second centrifugation. Thus, the first, short, centrifugation was obviously bringing down most intact bacteria and large cell debris but not the small cell fragments generated by heat killing. Most importantly, since almost all the radioactivity could be brought down eventually, this radioactivity must have remained associated with cell fragments. Thus, once again, the radiolabel was shown to be stable under the conditions of the study.

That the time of incubation had no effect on these results simply reflects the rapid binding kinetics of this phage to both live and heat-killed bacteria and fragments. To evaluate further the nature of the radioactivity remaining in suspension after incubation of the ^{99m}Tc -labeled phage at 37°C , in this case with live *E. coli* 2537 bacteria, after an initial spin the supernatants were subjected to $0.2\ \mu\text{m}$ filtration and C-18 HPLC analysis. As shown in Figure 3, after a 1 min centrifugation the supernatant contained 9% of the added radioactivity at 1 min of incubation, and that percentage increased to 33% at 105 min of incubation. Nevertheless, the percentage of radioactivity passing the filter re-

TABLE 1
 ^{99m}Tc -Phage Binding to Live and Heat-Killed Bacteria

Bacteria	Condition	Pellet	Supernatant
<i>E. coli</i> 2537	Live	71	24
	Heat killed	59	37
<i>S. aureus</i>	Live	86	9
	Heat killed	76	20
<i>E. coli</i> 25922	Live	83	12
	Heat killed	70	25

Data are added radioactivity in pellet and supernatant (%; mean of $n = 2$).

TABLE 2

Radioactivity in Supernatant After Serial Centrifugations with Time of Incubation at 37°C

Time	<i>E. coli</i> 2537	Supernatant	
		First spin (1 min at 850g)	Second spin (10 min at 850g)
1 min	Live	4	4
	Heat killed	36	6
15 min	Live	5	5
	Heat killed	14	5
60 min	Live	6	6
	Heat killed	21	7

Data are added radioactivity in supernatant (%), mean of $n = 2$.

mained constant at about 7% over time. Because the radioactivity removed by filtration was on particulates, almost certainly bacterial wall and membrane fragments, the increasing radioactivity in the supernatant with time of incubation can be explained by increased phage-mediated cell killing and generation of fragments not brought down by the centrifugation but removed by the filtration. Therefore, these data show that the label on bacteria was stable to incubation even after bacterial lysis.

The radioactivity in the filtrate was analyzed by reversed-phase C-18 HPLC. Figure 4 presents the radiochromatogram obtained by analyzing the 30 min incubate, with radiochromatograms of pertechnetate and ^{99m}Tc -MAG3 included for comparison. Each filtrate radiochromatogram showed a similar peak with a retention time identical to that of pertechnetate and was therefore most probably pertechnetate. The recovery was always greater than 90%.

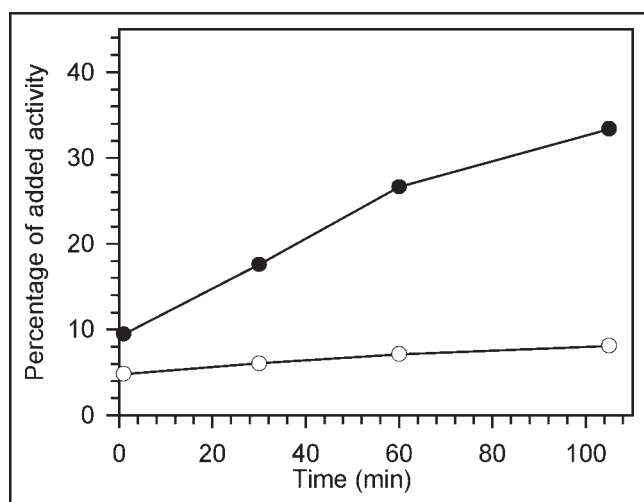


FIGURE 3. Percentage of added activity remaining in the supernatant following centrifugation after incubation of ^{99m}Tc -phage with *E. coli* 2537 (black circles) and in the same supernatant after 0.2 μm filtration (white circles). The decrease in activity after filtration demonstrates that the activity was associated with particles.

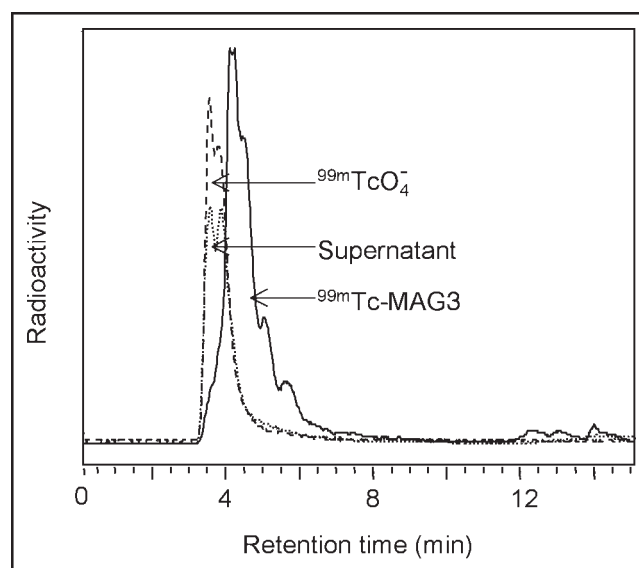


FIGURE 4. Reversed-phase C-18 HPLC radiochromatograms. Shown is the 0.2 μm filtrate of the 30 min supernatant after incubation of ^{99m}Tc -labeled phage with *E. coli* 2537. Included as standards are $^{99m}\text{TcO}_4^-$ and ^{99m}Tc -MAG3.

Biodistribution in Normal Mice

The biodistribution of the ^{99m}Tc -labeled phage in normal mice at various times is shown in Figure 5. The lungs and liver were the organs of greatest accumulation at the earliest time, with about 31% in liver, 8% in lungs, and 2% in spleen at 30 min. Activity in all organs gradually decreased over time such that at 6 h kidneys, spleen, and lungs contained only about 1% of the injected dose and by 24 h liver activity was reduced to 5% and lung activity to 0.39%. Values for blood were 2.5% at 30 min and decreased to 0.2% at 24 h. That the lung levels rapidly decreased with time suggests that localization in this organ was not simply due to capillary trapping of a radiolabeled particle. The unexpectedly high radioactivity levels in lungs at 30 min were not investigated further.

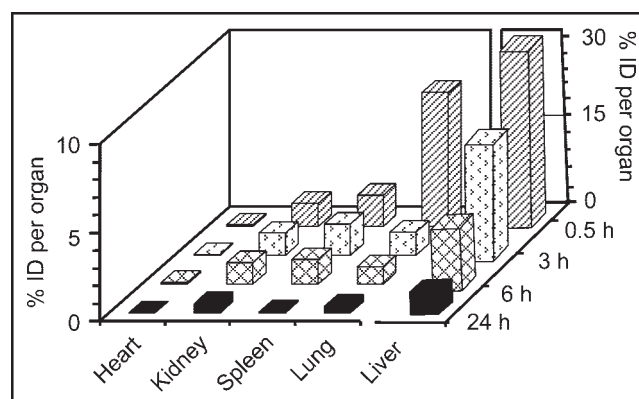


FIGURE 5. Radioactivity levels (percentage injected dose [% ID] per organ) of ^{99m}Tc -labeled phage in tissues of normal mice at 0.5, 3, 6, and 24 h after administration. Liver, the highest organ of accumulation, is shown on its own scale.

TABLE 3
Biodistribution 4 Hours After Administration of ^{99m}Tc -Phage to Mice Receiving Live Bacteria (Infection/Inflammation Model) or Heat-Killed Bacteria (Inflammation Model) 3 Hours Earlier

Tissue	<i>E. coli</i> 2537		<i>S. aureus</i>		<i>E. coli</i> 25922	
	Live	Heat killed	Live	Heat killed	Live	Heat killed
Liver	15.8 (0.33)	15.1 (3.02)	17.4 (1.34)	16.5 (1.14)	13.1 (1.43)	13.9 (1.48)
Heart	0.09 (0.0)	0.08 (0.01)	0.06 (0.01)	0.05 (0.01)	0.06 (0.00)	0.06 (0.01)
Kidney	1.31 (0.16)	1.35 (0.06)	1.08 (0.12)	1.06 (0.20)	1.12 (0.20)	1.06 (0.06)
Lung	1.77 (0.16)	2.38 (0.79)	0.74 (0.14)	0.55 (0.19)	1.30 (0.25)	1.0 (0.26)
Spleen	0.88 (0.08)	1.35 (0.82)	0.97 (0.18)	0.69 (0.18)	0.91 (0.16)	1.06 (0.19)
Stomach	12.6 (0.43)	12.3 (2.84)	15.2 (1.25)	9.17 (2.79)	12.2 (4.06)	14.7 (2.65)
Small intestine	5.29 (0.38)	6.85 (2.65)	7.33 (1.31)	5.46 (1.25)	4.97 (0.99)	3.61 (1.04)
Large intestine	8.02 (1.96)	6.46 (1.66)	6.79 (0.97)	12.6 (3.27)	10.1 (0.84)	11.9 (2.19)
Blood	1.38 (0.08)	1.25 (0.14)	1.0 (0.18)	0.82 (0.25)	1.06 (0.23)	1.05 (0.17)
Target thigh	0.69 (0.1)	0.5 (0.05)	0.76 (0.07)	0.40 (0.04)	0.79 (0.07)	0.52 (0.01)
Normal thigh	0.33 (0.04)	0.33 (0.04)	0.36 (0.02)	0.27 (0.04)	0.30 (0.05)	0.29 (0.03)

Data are percentage injected dose per organ or per milliliter of blood (mean of $n = 4$, with SD in parentheses).

Infection/Inflammation Model

Table 3 presents the biodistribution at 4 h after administration of the labeled phage in mice induced 3 h earlier with an infection/inflammation or an inflammation in one thigh using 1 of the 3 bacterial preparations, both as live and heat-killed preparations. As before, the liver was the organ of greatest accumulation of radioactivity in all cases. Radioactivity was also high in the stomach and in the small and large intestines, possibly because of the presence of endogenous bacteria in these organs. Activity was 2 to 2.5 fold higher in the infected/inflamed thigh than in the normal thigh for each of the 3 bacterial preparations, whereas the ratios for the inflamed thigh to the normal thigh were lower at 1.5 to 1.8.

Infection/inflammation and inflammation are compared in the bar graph of Figure 6. The difference in the percentage injected dose that accumulated in the infected thigh

versus inflamed thigh was significant in each case (Student t test), at 0.69 versus 0.50 for *E. coli* 2537 ($P = 0.046$), 0.76 versus 0.40 for *S. aureus* ($P = 0.00039$), and 0.79 versus 0.52 for *E. coli* 25922 ($P = 0.0037$).

In one study, the live bacteria and heat-killed preparation were introduced only 20 min before administration of the ^{99m}Tc -phage in an attempt to minimize the contribution from inflammation in the infected thigh. After 3 h, the accumulated activity was 2.3 fold higher in the infected thigh than in the normal thigh, whereas the ratio for inflamed thigh to normal thigh was 1.6. These values are essentially identical to those obtained using a 3 h period between induction and phage administration. The percentage injected dose in the normal thigh was again statistically identical ($P = 0.11$) for both sets of animals.

Images

Figure 7 presents whole-body images taken 3 h after administration of ^{99m}Tc -labeled phage to mice that had

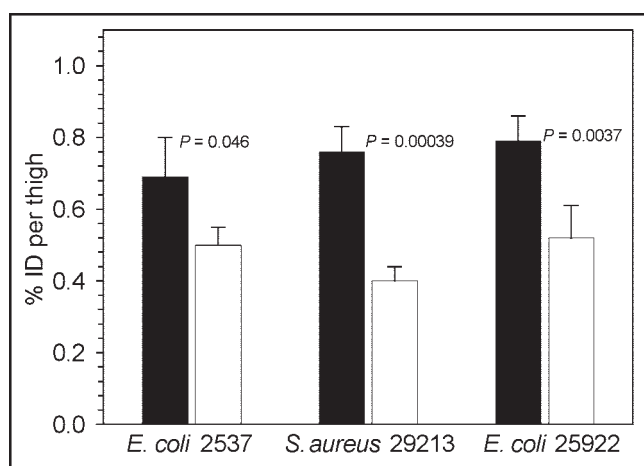


FIGURE 6. For the 3 bacterial preparations, comparison of activity (percentage injected dose [% ID]) in the infected thigh (black bars) and inflamed thigh (white bars) of mice, with the significance between the two indicated.

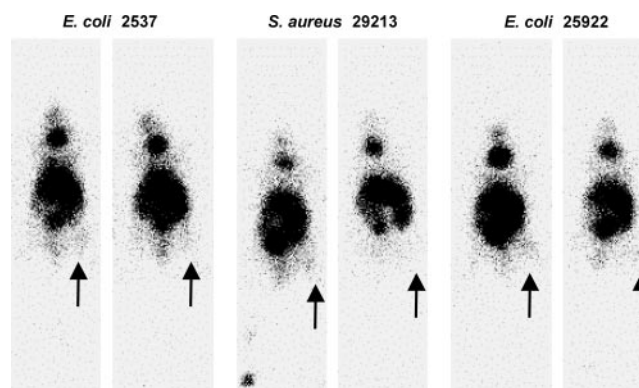


FIGURE 7. For the 3 bacterial preparations, whole-body images at 3 h after administration of ^{99m}Tc -MAG3 phage to mice with an infection (left panels) or inflammation (right panels) in the target thigh (arrows).

received the 3 bacterial preparations as either infection/inflammation or inflammation in the right thigh. The area of highest accumulation is in the abdomen, most likely liver and gut. The focal uptake in the neck is thought to be due to the small percentage of pertechnetate in the injectates localizing in the thyroid. The greater accumulation of activity in the infected thigh than in the inflamed thigh is evident.

DISCUSSION

Most agents considered for infection imaging are actually markers of inflammation and cannot discriminate between inflammation and infection. These include ^{67}Ga (16,17), ^{111}In or $^{99\text{m}}\text{Tc}$ -labeled leukocytes (18–20), polyclonal non-specific IgG(1), cytokines (21), liposomes (22), chemotactic peptides (23), human neutrophil elastase-2 (24), and streptavidin–biotin (25,26). Thus far, only $^{99\text{m}}\text{Tc}$ -Infecton, an antibiotic, and $^{99\text{m}}\text{Tc}$ -ubiquitin, a bacteria-specific peptide, have been presented as infection-specific imaging agents.

After their discovery in 1920, bacteriophages that replicate by lysing their bacterial host were considered an advancement in the treatment of bacterial infections (9). However, with the introduction of antibiotics, clinical use of phages to treat bacterial infections diminished, but phage therapy continues today in parts of Eastern Europe and is being reconsidered elsewhere in response to the growing occurrence of antibiotic-resistant bacteria (27). Phages have also been used for bacterial typing and as an epidemiologic tool (28).

To our knowledge, bacteriophages have not previously been considered as potential diagnostic agents. Because phages are bacterial specific and have been used in the clinic for infection therapy, apparently safely, for more than 80 y, their investigation as a potential infection-specific imaging agent appears reasonable, although their safety and efficacy remain to be evaluated. A potential limitation in this application may be the narrow specificity of phages. However, this limitation may simply require the use of a phage cocktail to include the more prevalent bacterial infections.

We have shown that the M13 phage may be labeled with $^{99\text{m}}\text{Tc}$ using MAG3 without in vitro evidence of label instability in saline or serum. We have also shown that the radiolabeled phage binds immediately and essentially equally to both live and heat-killed bacteria and that, once bound, the phage is surprisingly stable to dissociation. Furthermore, when we tested M13 binding to 3 different bacterial strains in culture, we observed a measure of specificity in that *E. coli* 2537 appeared to be preferred to *E. coli* 25922 and *S. aureus* 29213.

The biodistribution of phages in animals has not been exhaustively investigated. Inchely reported that the ^{51}Cr -labeled T4 phage immediately clears to the liver (29). While working with λ phage, Geier et al. found the phage titer to be highest in the spleen and to clear much more slowly from that organ than from other tissues (30). We observed the highest accumulation of radiolabeled phage in the liver and

gut, and a rapid accumulation of radioactivity in the lungs that also decreased rapidly. These differences are likely due to the use of different phages. The high levels of radioactivity accumulation in the stomach and gut may be due to targeting of endogenous bacteria in these organs and needs further investigation.

However, it is the result in infection that may be the most informative about the properties of radiolabeled phage. When tested in an infection/inflammation mouse model, the radiolabeled phage showed statistically significantly higher accumulations in the target thigh than in the normal contralateral thigh, regardless of the bacterial type used for infection. Although the expected higher accumulation was seen in the inflamed thigh of the inflammation mouse model than in the normal contralateral thigh, this accumulation was significantly lower than in the infection model. The increased accumulation in infection therefore argues in favor of a mechanism that, at least in part, involves specific binding to bacteria and is thus in agreement with our in vitro results showing bacterial binding.

CONCLUSION

We have presented evidence that a bacteriophage radiolabeled with $^{99\text{m}}\text{Tc}$ appears to bind to 3 types of bacteria in a manner that suggests the binding is specific. Further investigations are necessary to determine whether and to what extent these observations are general and pertain to other phages and other bacterial types. The results of this investigation suggest that further studies may be warranted to evaluate the potential of radiolabeled phages as bacteria-specific imaging agents. If further studies confirm that radiolabeled phages bind to bacterial fragments, then in contrast to other infection-imaging agents under development, radiolabeled phages may eventually be useful after antibiotic treatment.

REFERENCES

1. Rubin RH, Young LS, Hansen WP, et al. Specific and nonspecific imaging of localized Fisher immunotype 1 *Pseudomonas aeruginosa* infection with radiolabeled monoclonal antibody. *J Nucl Med*. 1988;29:651–656.
2. Vinjamuri S, Hall A, Britton KE. Tc99m Infecton, a bacterial specific infection imaging agent [abstract]. *Eur J Nucl Med*. 1995;22:916.
3. Vinjamuri S, Hall AV, Solanki KK, et al. Comparison of $^{99\text{m}}\text{Tc}$ Infecton imaging with radiolabeled white-cell imaging in the evaluation of bacterial infection. *Lancet*. 1996;347:233–235.
4. Britton KE, Vinjamuri S, Hall AV, et al. Clinical evaluation of technetium-99m Infecton for the localization of bacterial infection. *Eur J Nucl Med*. 1997;24:553–556.
5. Hall AV, Solanki KK, Vinjamuri S, Britton KE, Das SS. Evaluation of the efficacy of $^{99\text{m}}\text{Tc}$ -Infecton, a novel agent for detecting sites of infection. *J Clin Pathol*. 1998;51:215–219.
6. Nibbering PH, Welling M, Van Den Broek, Pauwels EKJ. Radiolabeled antimicrobial peptides for imaging of infections: a review. *Nucl Med Commun*. 1998;19:1117–1121.
7. Welling M, Paulusma-Annema M, Balter HS, Pauwels EKJ, Nibbering PH. Technetium-99m labeled antimicrobial peptides discriminate between bacterial infections and sterile inflammations. *Eur J Nucl Med*. 2000;27:292–301.
8. Welling M, Monguera S, Lupetti A, et al. Radiochemical and biological characteristics of $^{99\text{m}}\text{Tc}$ -UBI 29-41 for imaging of bacterial infections. *Nucl Med Biol*. 2002;29:413–422.

9. d'Herelle F. *The Bacteriophage: Its Role in Immunity*. Smith GH, trans. Baltimore, MD: Williams and Wilkins Co./Waverly Press; 1922.
10. Merrill CR, Scholl D, Adhya SL. The prospect for bacteriophage therapy in Western medicine. *Nat Rev Drug Discov*. 2003;2:489–497.
11. Winnard P Jr, Chang F, Rusckowski M, Mardirossian G, Hnatowich DJ. Preparation and use of NHS-MAG₃ for technetium-99m labeling of DNA. *Nucl Med Biol*. 1997;24:425–432.
12. PhD-12 Phage Display Peptide Library Kit. In: *New England Biolabs Manual*. Version 2.5. Beverly, MA: New England Biolabs, Inc.; 1999:1–23.
13. Smith GP, Scott JK. Libraries of peptides and proteins displayed on filamentous phage. *Meth Enzymol*. 1993;217:228–257.
14. Hnatowich DJ, Qu T, Chang F, Ley AC, Ladner RC, Rusckowski M. Labeling peptides with ^{99m}Tc using an NHS-MAG₃ bifunctional chelator. *J Nucl Med*. 1998;39:56–64.
15. Brock TD. *Biology of Microorganisms*. Englewood Cliffs, NJ: Prentice-Hall Inc.; 1970:206.
16. Lavender JP, Lowe J, Barker JR, Burn JL, Chaudhri MA. Gallium-67 citrate scanning in neoplastic and inflammatory lesions. *Br J Radiol*. 1971;44:361–366.
17. Weiner RE. The mechanism of ⁶⁷Ga localization in malignant disease. *Nucl Med Biol*. 1996;23:745–751.
18. McAfee JG, Thakur ML. Survey of radioactive agents for the in vitro labeling of phagocytic leucocytes. I. Soluble agents. *J Nucl Med*. 1976;17:480–487.
19. McAfee JG, Thakur ML. Survey of radioactive agents for the in vitro labeling of phagocytic leucocytes. II. Particles. *J Nucl Med*. 1976;17:488–492.
20. Peters AM, Danpure HJ, Osman S, et al. Preliminary clinical experience with ^{99m}Tc hexamethylpropylene-amineoxime for labeling leucocytes and imaging infection. *Lancet*. 1986;2:945–949.
21. Chianelli M, Signore A, Ronga G, Fritzberg A, Mather SL. Labeling, purification and biodistribution of ^{99m}Tc-interleukin-2: a new radiopharmaceutical for in vivo detection of activated lymphocytes [abstract]. *Eur J Nucl Med*. 1994;21:807.
22. Oyen WJG, Boerman OC, Storm G, et al. Detecting infection and inflammation with technetium-99m-labeled stealth liposomes. *J Nucl Med*. 1996;37:1392–1397.
23. Fischman AJ, Pike MC, Kroon D, et al. Imaging focal sites of bacterial infection in rats with indium-111-labeled chemotactic peptide analogs. *J Nucl Med*. 1991;32:483–491.
24. Rusckowski M, Qu T, Pullman J, et al. Inflammation/infection imaging with a ^{99m}Tc-neutrophil elastase inhibitor in monkeys. *J Nucl Med*. 2000;41:363–374.
25. Rusckowski M, Fritz B, Hnatowich DJ. Localization of infection using streptavidin and biotin: an alternative to nonspecific polyclonal immunoglobulin. *J Nucl Med*. 1992;33:1810–1815.
26. Fogarasi M, Pullman J, Winnard P, Hnatowich DJ, Rusckowski M. Pretargeting of bacterial endocarditis in rats with streptavidin and ¹¹¹In-labeled biotin. *J Nucl Med*. 1999;40:484–490.
27. Merrill CR, Biswas B, Carlton R, et al. Long-circulating bacteriophage as anti-bacterial agents. *Proc Natl Acad Sci*. 1996;93:3188–3192.
28. Ackermann HW, DuBow MS. *General Properties of Bacteriophages*. Boca Raton, FL: CRC Press; 1987:146. *Virus of Prokaryotes*; vol 1.
29. Inchley CJ. The activity of mouse Kupffer cells following intravenous injection of T4 bacteriophage. *Clin Exp Immunol*. 1969;5:173–187.
30. Geier MR, Trigg ME, Merrill CR. Fate of bacteriophage lambda in non-immune germ-free mice. *Nature*. 1973;246:221–222.





The Journal of
NUCLEAR MEDICINE

Investigations of a ^{99m}Tc -Labeled Bacteriophage as a Potential Infection-Specific Imaging Agent

Mary Rusckowski, Suresh Gupta, Guozheng Liu, Shuping Dou and Donald J Hnatowich

J Nucl Med. 2004;45:1201-1208.

This article and updated information are available at:
<http://jnm.snmjournals.org/content/45/7/1201>

Information about reproducing figures, tables, or other portions of this article can be found online at:
<http://jnm.snmjournals.org/site/misc/permission.xhtml>

Information about subscriptions to JNM can be found at:
<http://jnm.snmjournals.org/site/subscriptions/online.xhtml>

The Journal of Nuclear Medicine is published monthly.
SNMMI | Society of Nuclear Medicine and Molecular Imaging
1850 Samuel Morse Drive, Reston, VA 20190.
(Print ISSN: 0161-5505, Online ISSN: 2159-662X)

© Copyright 2004 SNMMI; all rights reserved.